

Supplementary Material for:

Asymmetric phonon-drag effect and thermoelectric performance in PbTe under strain modulation

Yao Liu, Yu-Jia Zeng^a, Wu-Xing Zhou^b

School of Materials Science Engineering, Hunan University of Science and Technology, Xiangtan 411201, China

a) [Authors to whom correspondence should be addressed: zengyujia@hnust.edu.cn](mailto:zengyujia@hnust.edu.cn)

b) Authors to whom correspondence should be addressed: wuxingzhou@hnu.edu.cn

1. Strain-dependent electronic and phonon structures

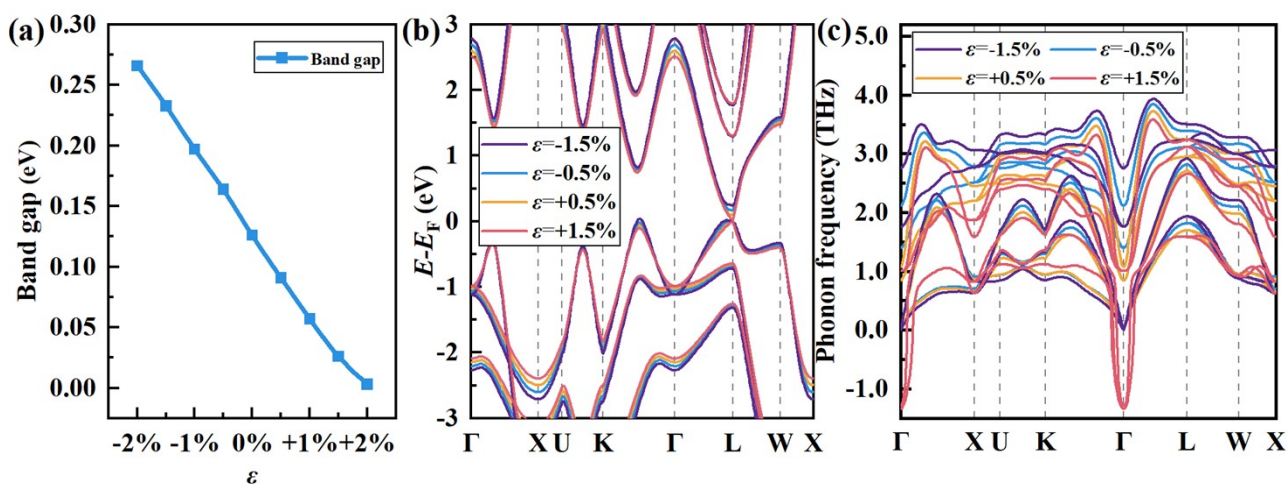


Fig. S1. Strain-dependent electronic and phonon structures of PbTe. (a) Calculated band gap of PbTe as a function of isotropic strain from -2.0% to $+2.0\%$. (b) Electronic band structures under four representative strain conditions, $\epsilon = -1.5\%$, -0.5% , $+0.5\%$, and $+1.5\%$, plotted along the high-symmetry paths. The dashed vertical lines indicate the high-symmetry points. (c) Phonon dispersion curves of PbTe at $\epsilon = -1.5\%$, -0.5% , $+0.5\%$, and $+1.5\%$. Negative frequencies indicate imaginary modes. The results show phonon hardening under compressive strain and low-frequency phonon softening under tensile strain. In addition, the band structure at $\epsilon = -1.5\%$ shows that the Σ valley shifts upward and exceeds the L point, becoming the new valence-band maximum.

Fig. S1 summarizes the strain-dependent evolution of the electronic and phonon structures of PbTe. As shown in Fig. S1(a), the band gap changes continuously within the studied strain range, increasing under compressive strain and decreasing under tensile strain. The representative band structures in Fig. S1(b) further show that strain not only tunes the band gap but also changes the relative positions of different valence valleys near the Fermi level. In particular, at $\epsilon = -1.5\%$, the Σ valley shifts upward and exceeds the L point, becoming the new valence-band maximum. This indicates that stronger compressive strain

induces a change in the electronic structure near the Fermi level that is distinct from the mildly compressed cases. This electronic-structure change provides a basis for understanding the enhanced electron–phonon scattering and phonon-drag correction at $\varepsilon = -1.5\%$.

Fig. S1(c) shows the phonon dispersions under representative strain conditions. Compressive strain hardens the phonon branches, whereas tensile strain softens the low-frequency phonon modes. At $\varepsilon = +1.5\%$, an imaginary mode appears near the Γ point, indicating dynamical instability. Similar soft-mode behavior has been reported in previous first-principles studies. Murphy et al. showed that tensile strain can drive PbTe close to the ferroelectric phase-transition boundary; at a tensile strain of $\eta = 1.15\%$, one Γ -point TO mode softens significantly from approximately 1 THz in the equilibrium structure to about 0.1 THz, indicating that PbTe is highly sensitive to tensile strain and approaches the soft-mode instability regime [ref. 22]. Therefore, the imaginary mode observed under isotropic tensile strain of $\varepsilon = +1.5\%$ in this work is physically reasonable and reflects the proximity of PbTe to a soft-mode instability.

Since reliable Boltzmann transport calculations require dynamically stable phonon spectra, $\varepsilon = +1.5\%$ and larger tensile strains were not used for subsequent transport calculations. On the compressive side, $\varepsilon = -1.5\%$ remains dynamically stable and was therefore included as a stronger-compression case to examine the effect of electronic-structure changes near the Fermi level on electron–phonon scattering and phonon drag. We did not further perform fully coupled drag/no-drag transport calculations at $\varepsilon = -2.0\%$ for two reasons. First, fully coupled electron–phonon BTE calculations are computationally expensive. Second, $\varepsilon = -1.5\%$ already shows a clear transfer of the valence-band maximum from the L point to the Σ valley, together with a pronounced enhancement of phonon drag, which is sufficient to indicate a drag-enhancement source under stronger compression that is different from the tensile softening mechanism. Therefore, the following supplementary transport analysis focuses on the representative dynamically stable strain states of $\varepsilon = -1.5\%$, -1% , -0.5% , 0 , $+0.5\%$, and $+1\%$.

2. Phonon and electron scattering under $\varepsilon = -1.5\%$ compressive strain

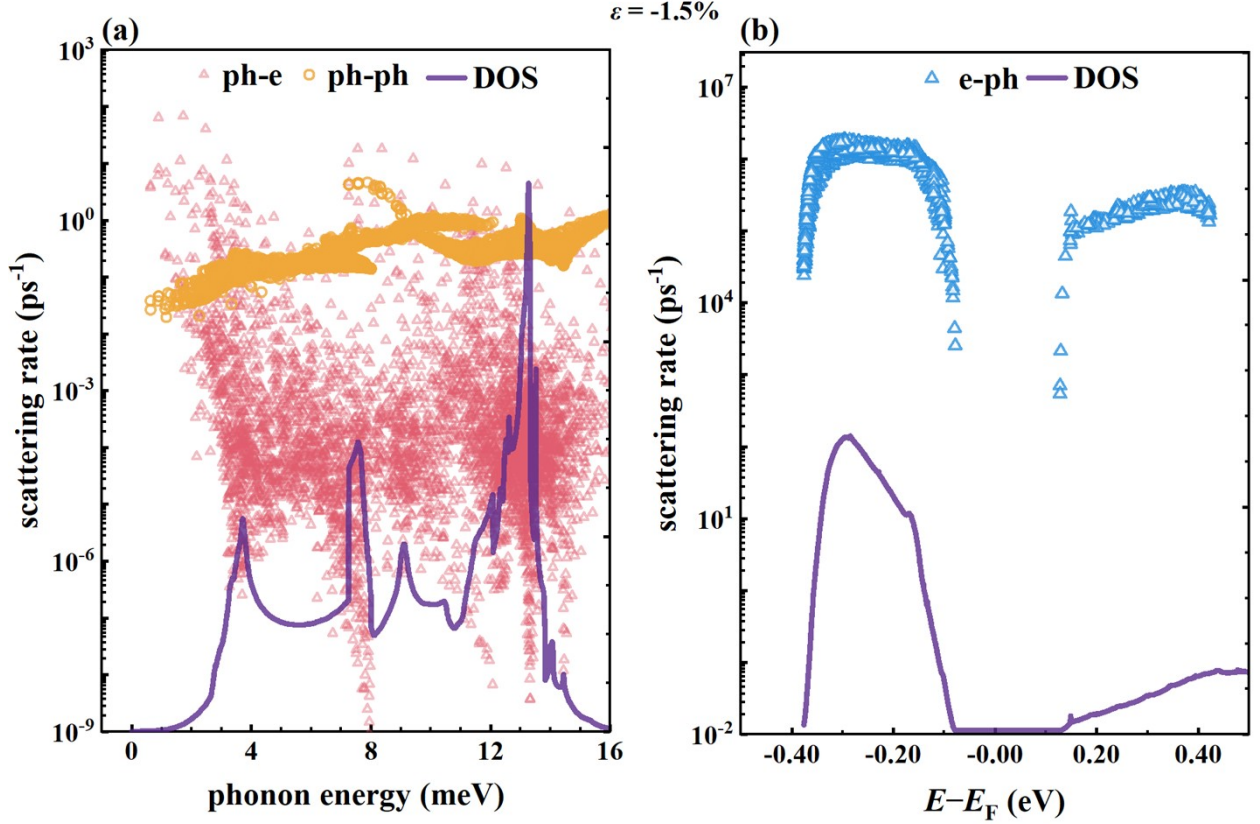


Fig. S2. Phonon and electron scattering properties of PbTe under $\varepsilon = -1.5\%$ compressive strain at 300 K. (a) Phonon scattering rates as a function of phonon energy. Pink open triangles, orange open circles, and the purple solid line represent the phonon–electron (ph-e) scattering rate, phonon–phonon (ph-ph) scattering rate, and phonon DOS, respectively. (b) Electron–phonon (e-ph) scattering rates as a function of electronic energy. Blue open triangles and the purple solid line represent the e-ph scattering rate and electronic DOS, respectively.

At $\varepsilon = -1.5\%$, the ph-e scattering rate is significantly enhanced over a wide phonon-energy range and reaches a magnitude comparable to, or even higher than, the ph-ph scattering rate in some regions. Meanwhile, the phonon DOS shifts overall toward the high-energy region, indicating phonon-mode hardening induced by compressive strain. Therefore, the enhanced ph-e scattering under this strain condition is different from the soft-phonon mechanism under $\varepsilon = +1\%$ tensile strain.

The electron-side scattering is also strongly enhanced. The e-ph scattering rates remain high on both the valence- and conduction-band sides, while the gap between them corresponds to the enlarged band gap under this strain condition. Since the electronic DOS does not show a corresponding increase compared with the results in Fig. 2, the enhancement of the e-ph scattering rate is more likely related to changes in electronic scattering channels rather than to an increase in the electronic DOS itself. As shown in Fig. S1(b), under $\varepsilon = -1.5\%$, the Σ valley shifts upward and exceeds the L point, becoming the new valence-band maximum. Previous first-principles studies of p-type PbTe have shown that the relative positions of the L and Σ valleys and the L– Σ intervalley scattering channels play important roles in thermoelectric transport [ref.6]. Because the Σ valley has a higher valley degeneracy, its participation in band-edge transport increases the available electronic initial and final states near the Fermi level and provides additional channels for electron–phonon scattering processes that satisfy energy and momentum conservation. Therefore, the enhanced ph-e and e-ph scattering under $\varepsilon = -1.5\%$ is more likely associated with compression-induced changes in the band-edge electronic structure.

3. Strain dependence of drag and no-drag Seebeck coefficients

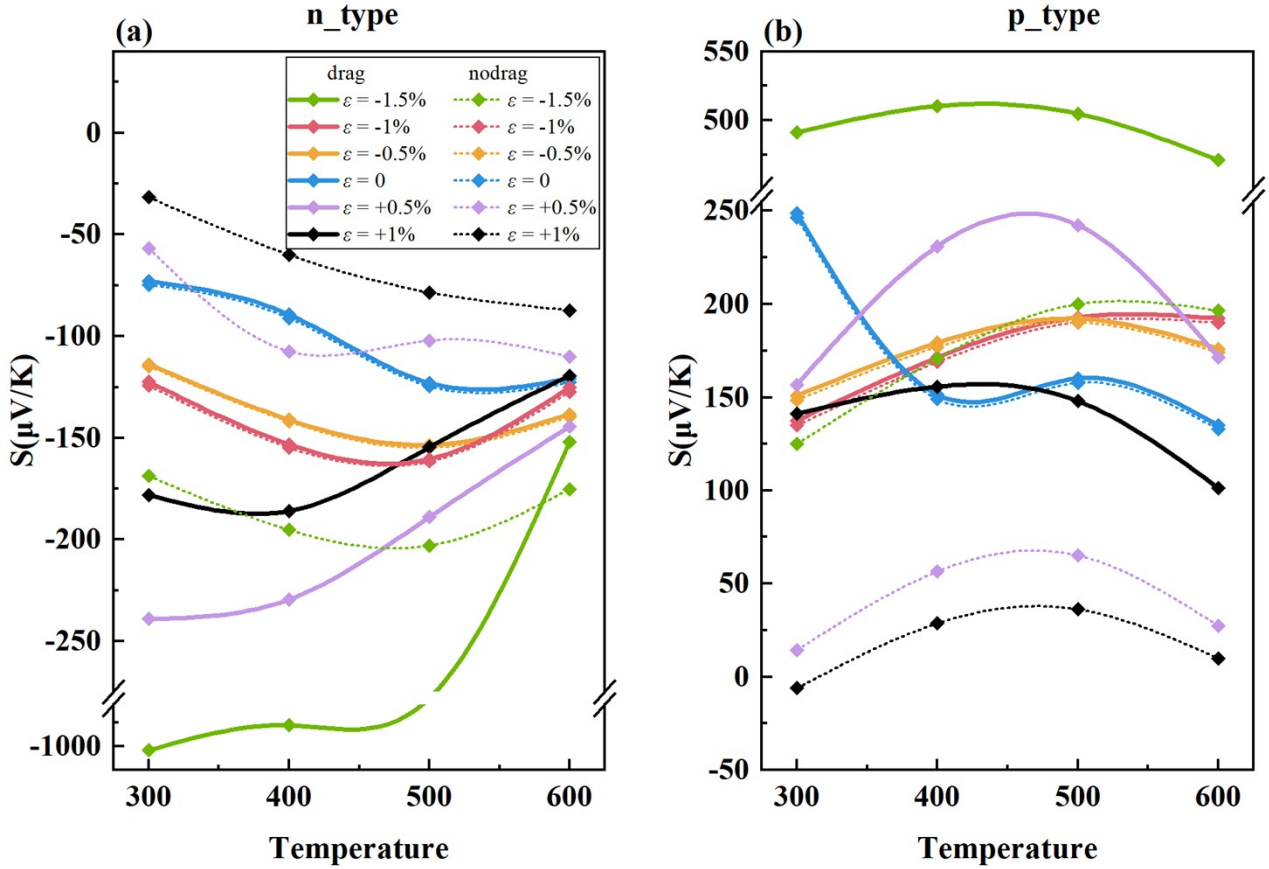


Fig. S3. Strain dependence of drag and no-drag Seebeck coefficients. Temperature-dependent Seebeck coefficients of PbTe under representative dynamically stable strain conditions. (a) n-type PbTe with $n_e = 1 \times 10^{19} \text{ cm}^{-3}$. (b) p-type PbTe with $n_h = 1 \times 10^{20} \text{ cm}^{-3}$. Solid lines denote the fully coupled electron–phonon Boltzmann transport results, referred to as the drag results, whereas dotted lines denote the decoupled electron and phonon Boltzmann transport results, referred to as the no-drag results. Different colors represent $\epsilon = -1.5\%$, -1% , -0.5% , 0 , $+0.5\%$, and $+1\%$.

Fig. S3 compares the Seebeck coefficients of PbTe obtained from drag and no-drag calculations under representative dynamically stable strain conditions. The selected strain states were determined by considering phonon dynamical stability and the high computational cost of fully coupled electron–phonon BTE calculations. As shown in Fig. S1(c), an imaginary phonon mode appears at $\epsilon = +1.5\%$, indicating dynamical instability. Therefore, this strain state and larger tensile strains, such as $+2.0\%$, are not suitable for Boltzmann transport calculations. The $\epsilon = -1.5\%$ case remains dynamically stable and is included as a stronger-compression case to examine whether phonon drag can also be enhanced beyond the mildly compressed regime.

For both n-type and p-type PbTe, the drag and no-drag results are close at $\epsilon = -1\%$, -0.5% , and 0 , indicating that the phonon-drag correction to the Seebeck coefficient is weak under the unstrained and mildly compressed conditions. In contrast, a clear difference between the drag and no-drag results appears on the tensile-strain side, especially at $\epsilon = +0.5\%$ and $+1\%$. For n-type PbTe, the fully coupled drag calculation increases the magnitude of the negative Seebeck coefficient. For p-type PbTe, the no-drag calculation strongly suppresses the Seebeck coefficient under tensile strain, whereas the drag calculation maintains a much larger positive Seebeck coefficient. This indicates that the phonon-drag contribution is already activated at $\epsilon = +0.5\%$ and remains significant at $\epsilon = +1\%$, rather than being an isolated result at $\epsilon = +1\%$.

Notably, the stronger-compression case of $\varepsilon = -1.5\%$ also shows a pronounced drag correction, especially at low temperature. This result indicates that phonon drag in PbTe is not simply a tensile-only effect. Combined with the electronic and phonon structure evolution in Fig. S1 and the scattering analysis in Fig. S2, the enhanced phonon drag under tensile strain is mainly associated with band-gap narrowing and low-frequency phonon softening, whereas the enhancement under $\varepsilon = -1.5\%$ is accompanied by the upward shift of the Σ valley to the valence-band maximum and markedly enhanced electron-phonon scattering. Therefore, Fig. S3 confirms the asymmetric strain regulation of phonon drag in PbTe: the drag contribution is weak under the unstrained and mildly compressed conditions, becomes significant under tensile strain, and can also be enhanced under stronger compression through a mechanism distinct from the tensile-side soft-phonon mechanism.

4. Validation of Wannier interpolation

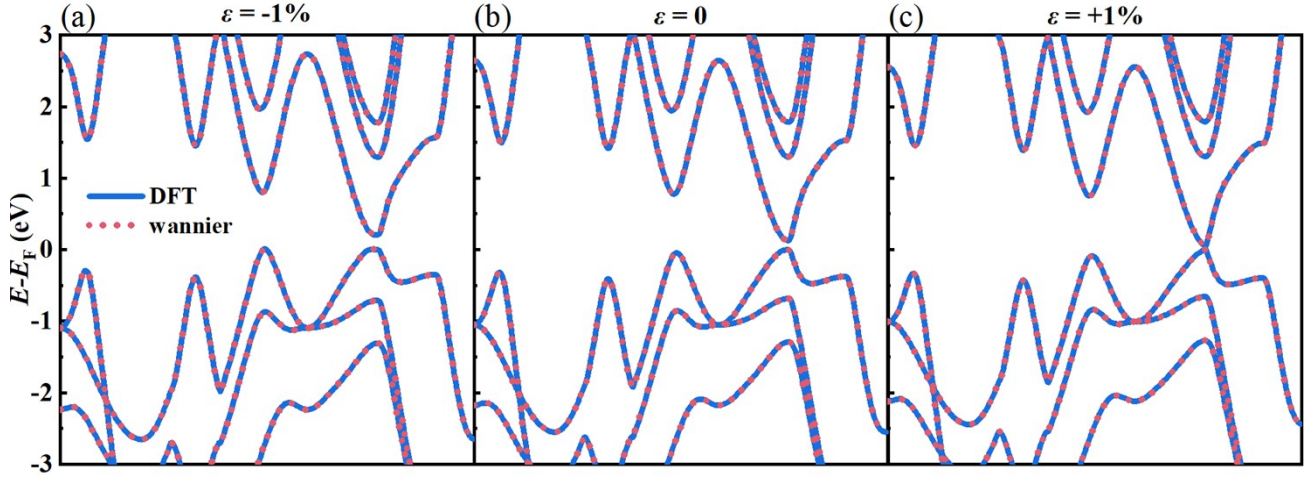


Fig. S4. Electronic band structures of PbTe within ± 3 eV of the Fermi level under $\varepsilon = -1\%$, 0 , and $+1\%$. Solid blue lines denote the DFT bands, and dotted red lines denote the Wannier-interpolated bands. The good agreement near the band edges supports the reliability of the Wannier interpolation for the subsequent electron–phonon coupling and transport calculations.

Fig. S4 validates the Wannier interpolation used in the electron–phonon coupling and transport calculations. The Wannier-interpolated bands reproduce the original DFT band structures well under all three strain conditions, especially near the band edges and around the L valley, which are most relevant to the thermoelectric transport of PbTe. This agreement indicates that the Wannier tight-binding model accurately captures the electronic states involved in carrier transport. Therefore, the subsequent EPW electron–phonon coupling interpolation and elphbolt Boltzmann transport calculations are based on a reliable electronic structure representation.